ISSN (Print) : 2320 – 3765
ISSN (Online): 2278 – 8875

International Journal of Advanced Research in Electrical, Electronics and Instrumentation Engineering

(A High Impact Factor, Monthly, Peer Reviewed Journal, (An UGC Approved Journal))

Website: www.ijareeie.com

Vol. 6, Issue 9, September 2017

Synthesis, Characterization and Application of Zinc-Oxide nanoparticles of special morphology in Hybrid Solar Cells

Somnath Middya*

*Department of Physics, Bankim Sardar College, South 24 Parganas, India

ABSTRACT: Zinc Oxide (ZnO) holds significant importance in optoelectronic and photovoltaic applications, promise across various technological fields due to its stability, wide band gap, and semiconductor behavior. Recognized as a non-toxic n-type wide bandgap semiconductor [1], ZnO has found efficient applications in thin film transistors [2], light-emitting diodes [3,4], optical sensors [5-8], and photovoltaics [9-11]. The material's wide band gap and high exciton binding energy (60 meV) [12], coupled with excellent optical transparency [13], position it as a promising candidate for the construction of organic-inorganic hybrid solar cells [14,15]. The substantial excitonic binding energy of ZnO contributes to exceptional exciton stability, even at elevated temperatures [16], enabling devices to operate at low threshold voltages. Another crucial characteristic of ZnO nanoparticles is the tenability of electron mobility [17], achievable by optimizing particle shape and size. Tailoring the morphology of semiconducting nanoparticles and adjusting doping concentration [18, 19] allows for the preparation of nanomaterials with a suitable band gap for specific device applications. Depending on the morphological growth of semiconducting nanoparticles and doping concentration [18, 19], the absorption edge can be shifted to higher energies, populating all states near the conduction band. This results in a higher band gap, making the material more adept at transitioning excitons above room temperature. Considerable efforts have been invested in synthesizing Zinc Oxide (ZnO) nanoparticles with diverse morphologies. Zhang et al. [20] reported the existence of flower-shaped, prism-like, rod-like, and snowflake-like ZnO nanoparticles. Gao et al. demonstrated the synthesis of flower-like ZnO using the thermolysis technique [21]. Yang et al. presented a synthesis method for flower-shaped, disk-shaped, and dumbbell-like ZnO structures, assisted by capping molecules like citric acid and polyvinyl alcohol [22].This Experiment focuses on investigating the structural behavior of ZnO in MEH-PPV/ZnO-based organic-inorganic hybrid solar cells. For this study, we have included sphere-like, rod-like, and flower-like ZnO nanoparticles. Specifically, the synthesis of flower-like ZnO nanoparticles is detailed in this chapter, employing the solvothermal technique with the capping reagent TOAB (tetra-octyl ammonium bromide). The material characterization of the flower-like ZnO is outlined in the following sections.

I. INTRODUCTION

Zinc Oxide (ZnO) holds significant importance in optoelectronic and photovoltaic applications, showcasing promise across various technological fields due to its stability, wide band gap, and semiconductor behavior. Recognized as a non-toxic n-type wide bandgap semiconductor [1], ZnO has found efficient applications in thin film transistors [2], light-emitting diodes [3,4], optical sensors [5-8], and photovoltaics [9-11]. The material's wide band gap and high exciton binding energy (60 meV) [12], coupled with excellent optical transparency [13], position it as a promising candidate for the construction of organic-inorganic hybrid solar cells [14,15]. The substantial excitonic binding energy of ZnO contributes to exceptional exciton stability, even at elevated temperatures [16], enabling devices to operate at low threshold voltages. Another crucial characteristic of ZnO nanoparticles is the tunability of electron mobility [17], achievable by optimizing particle shape and size. Tailoring the morphology of semiconducting nanoparticles and adjusting doping concentration [18, 19] allows for the preparation of nanomaterials with a suitable band gap for specific device applications. Depending on the morphological growth of semiconducting nanoparticles and doping concentration [18, 19], the absorption edge can be shifted to higher energies, populating all states near the conduction band. This results in a higher band gap, making the material more adept at transitioning excitons above room

ISSN (Print) : 2320 – 3765
ISSN (Online): 2278 – 8875

International Journal of Advanced Research in Electrical, Electronics and Instrumentation Engineering

(A High Impact Factor, Monthly, Peer Reviewed Journal, (An UGC Approved Journal))

Website: www.ijareeie.com

Vol. 6, Issue 9, September 2017

temperature. Considerable efforts have been invested in synthesizing Zinc Oxide (ZnO) nanoparticles with diverse morphologies. Zhang et al. [20] reported the existence of flower-shaped, prism-like, rod-like, and snowflake-like ZnO nanoparticles. Gao et al. demonstrated the synthesis of flower-like ZnO using the thermolysis technique [21]. Yang et al. presented a synthesis method for flower-shaped, disk-shaped, and dumbbell-like ZnO structures, assisted by capping molecules like citric acid and polyvinyl alcohol [22].This Experiment focuses on investigating the structural behavior of ZnO in MEH-PPV/ZnO-based organic-inorganic hybrid solar cells. For this study, we have included sphere-like , rod-like, and flower-like ZnO nanoparticles. Specifically, the synthesis of flower-like ZnO nanoparticles is detailed in this chapter, employing the solvothermal technique with the capping reagent TOAB (tetra-octyl ammonium bromide). The material characterization of the flower-like ZnO is outlined in the following sections.

II. SYNTHESIS OF FLOWER SHAPED ZNO

2.1. Experimental Reagents

For the fabrication of flower-like zinc oxide (ZnO) nanoparticles, Merck was the source for acquiring anhydrous zinc acetate (Zn(COOH)2·2H2O), methanol, and AR-grade sodium hydroxide (NaOH) pellets. The organic capping reagent, tetra-octyl ammonium bromide (TOAB), was obtained from Sigma Aldrich.

2.2. Synthesis of ZnO nano flowers

The typical synthesis of ZnO nano flowers, the solvothermal technique was adopted. In this part, TOAB was used as the capping reagent.

III. MATERIAL CHARACTERIZATIONS

3.1. X-Ray Diffraction (XRD) Analysis

In analytical measurements, XRD pattern of the synthesized was recorded with the help of Bruker D8 X-Ray Diffractometer. In production of X-Ray Copper target was selected for CuKα radiation (λ = 0.15418 nm).The recorded XRD spectra for the flower like ZnO is given in Figure 1(c).

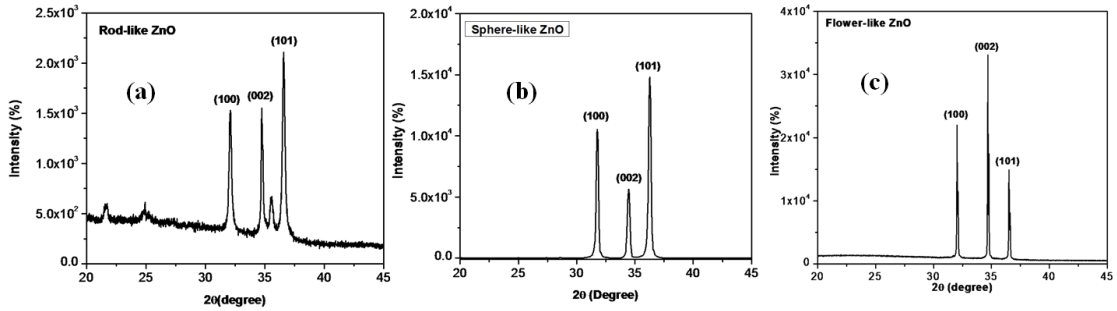

Figure 1: XRD image of ZnO

The X-ray diffraction (XRD) spectra, when recorded, revealed the prominent crystallographic planes (hkl) of ZnO nanoparticles, namely (100), (002), and (101), detected at angles 2θ = 32, 34.6, and 36.4 degrees, respectively. The diffraction patterns were consistent with the JCPDS Card No: 36-1451 [23], supporting the synthesized nanomaterials' various morphologies.

Notably, the intensity variation was particularly conspicuous for the (002) plane, suggesting potential influences from morphological growth. Utilizing the XRD data from Figure 1(c) and employing Scherrer's broadening equation, the average particle size of the ZnO flower-like nanoparticles was calculated to be 86 nm [24]. It was evident that all particles fell within the nanoscale range, ranging between 10-100 nm.

ISSN (Print) : 2320 – 3765
ISSN (Online): 2278 – 8875

International Journal of Advanced Research in Electrical, Electronics and Instrumentation Engineering

(A High Impact Factor, Monthly, Peer Reviewed Journal, (An UGC Approved Journal))

Website: www.ijareeie.com

Vol. 6, Issue 9, September 2017

3.2. Scanning Electron Microscopy (SEM) Analysis

Figure 2 displays the morphological structures of the synthesized material through a scanning electron microscope (SEM). The SEM image provides the distinctive characteristics of the flower-like morphology in the nano dimension. The architectural development of the nanoparticles is intricately linked to the solubility of the precursor in solvents with varying saturated vapor pressures and the initial nucleation of crystals [25, 26]. The water-soluble surfactant TOAB establishes a coordinate bond with Zn ions on the developing particles, facilitating the formation of the flower-like structure [27]. Furthermore, the chain length of the surfactant TOAB plays a role in influencing the crystal growth of the material.

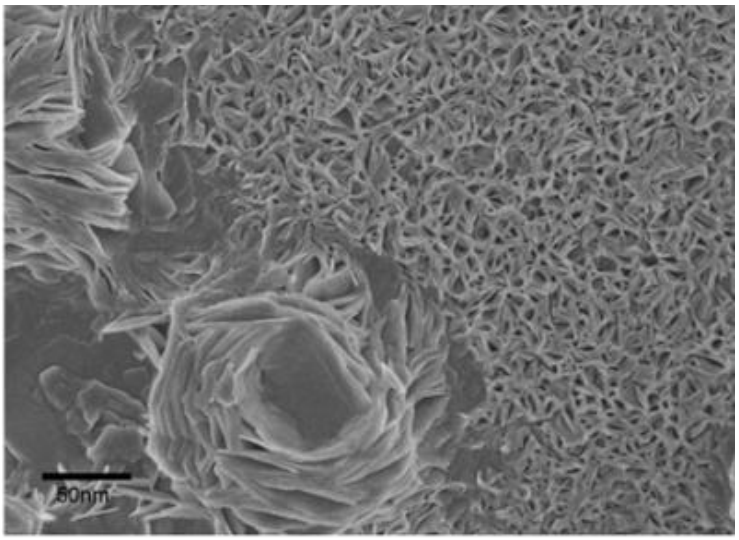

Figure 2: SEM image of ZnO flower

3.3. Fourier Transformed Infra-Red Spectroscopy of the synthesized Zinc-Oxides

The Fourier transform infrared spectra of ZnO, featuring distinct morphologies, were captured using the FTIR-8400S Spectrophotometer by Shimadzu (Figure 3). The investigation of functional groups was carried out through the analysis of FTIR spectroscopic data. To delineate the presence of specific functional groups, the Fourier transformation infrared spectra of ZnO nanoparticles with varied morphologies were recorded, and the resulting spectra are outlined below:

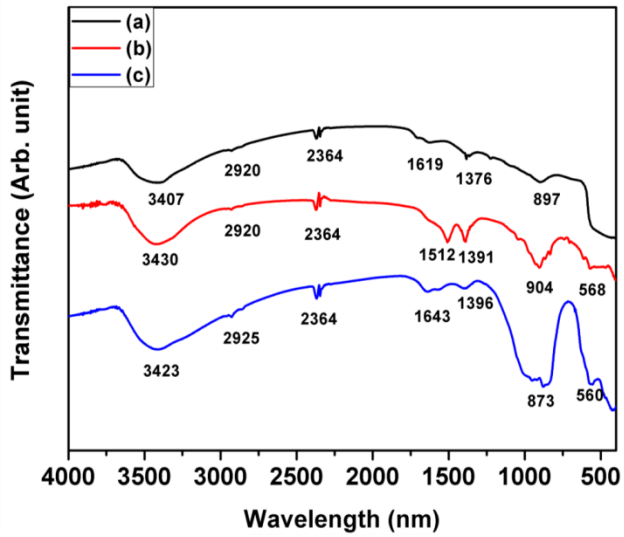

Figure 3: FTIR spectra of (a) ZnO rod, (b) ZnO sphere and (c) ZnO flower

ISSN (Print) : 2320 – 3765
ISSN (Online): 2278 – 8875

International Journal of Advanced Research in Electrical, Electronics and Instrumentation Engineering

(A High Impact Factor, Monthly, Peer Reviewed Journal, (An UGC Approved Journal))

Website: www.ijareeie.com

Vol. 6, Issue 9, September 2017

This spectra shows strong peak around 3400cm^{-1} to 3430 cm^{-1} for O-H stretching and a small peak around 2925 to 2920 cm^{-1} corresponding to C-H stretching for each samples. Peaks around 1650 to 1500 cm^{-1} and 1400 to 1370cm^{-1} indicated the formation of ZnO [28] and symmetric stretching of carboxylate group (COO-) probably from the un-reacted acetate. Peaks at around 560 cm^{-1} show the distinct stretching vibration of Zn-O.

IV. OPTICAL CHARACTERIZATIONS

4.1. UV-vis Absorption Analysis

The UV-vis Absorption spectra of the synthesized flower-like ZnO is given in Figure 5(c). Figure 5(a) and 5(b) represents the UV-vis absorption spectra of ZnO sphere and rod like morphology. Here we also introduced these two to compute the difference of flower-like ZnO with sphere and rod-like ZnO.

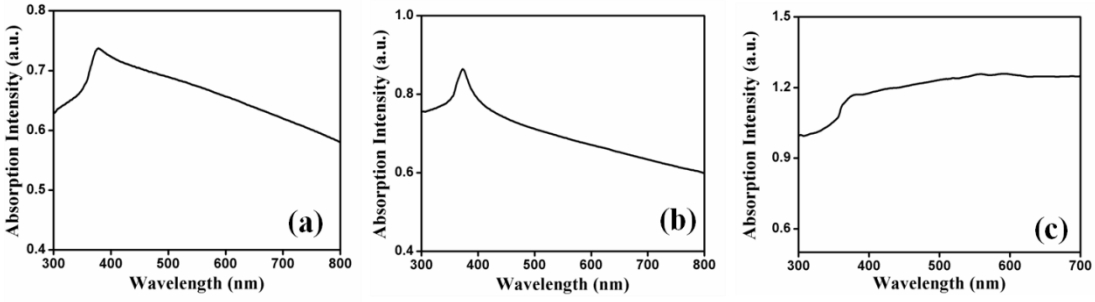

Figure 5: UV-vis absorption spectra of (a) ZnO rod, (b) ZnO sphere and (c) ZnO flower

It is evident that the sphere-like nanoparticle (Figure 5(b)) exhibits a peak at a lower wavelength, indicative of higher energy. Conversely, for rod-like and flower-like ZnO, there is a red shift, with absorption peaks shifting towards higher wavelengths.

4.1.1. Optical energy band gap estimation

Utilizing the data from Figure 5(c), the direct optical band gap of the flower-like ZnO was calculated with Tauc's equation, resulting in an estimated value of 3.86 eV (Figure 6(c)). Conversely, the sphere-like nano morphology displays high absorption due to its lower band gap, as evidenced by the absorption peak.

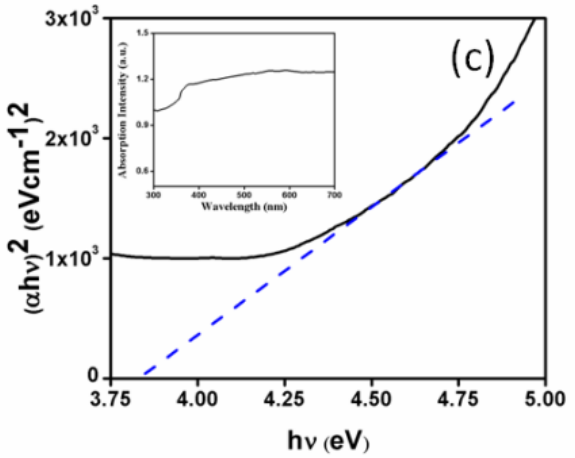

Figure 6: Tauc's plot of ZnO flower (c).

ISSN (Print) : 2320 – 3765
ISSN (Online): 2278 – 8875

International Journal of Advanced Research in Electrical, Electronics and Instrumentation Engineering

(A High Impact Factor, Monthly, Peer Reviewed Journal, (An UGC Approved Journal))

Website: www.ijareeie.com

Vol. 6, Issue 9, September 2017

The direct band gap energy underwent significant changes in the sphere and rod-like structures of ZnO, influenced by their morphological variations. This alteration may be attributed to the increased populations of states near the conduction band. Consequently, it can be concluded that the sphere-like structure is more suitable for high-temperature applications in hybrid solar cells with organic polymers.

4.3. Optical Characterization of MEH-PPV

Before incorporating MEH-PPV into a device, thorough characterization was essential to gain detailed insights. To optimize the photo-sensing behavior of the acquired polymer, a solution of 1.5 mg/mL MEH-PPV in chloroform was prepared. UV-VIS absorption spectra of the MEH-PPV stock solution were then recorded in the wavelength range of 300 nm to 700 nm using a spectrophotometer (Figure 7). The spectrum reveals an excitation peak at 557 nm. The corresponding band gap energy was calculated using the equation Eg=1242/λpeak, resulting in a value of 2.21 eV [38]. The absorption coefficient and band gap of MEH-PPV, measured from Tauc's plot, further substantiated this value. The extrapolated part of the linear curve intersected at an incident photon energy of 2.22 eV, as depicted in Figure 7. Yuh-Zheng Lee et al. estimated the band gap energy of MEH-PPV as 2.1 eV by optimizing the HOMO and LUMO energy levels [39].

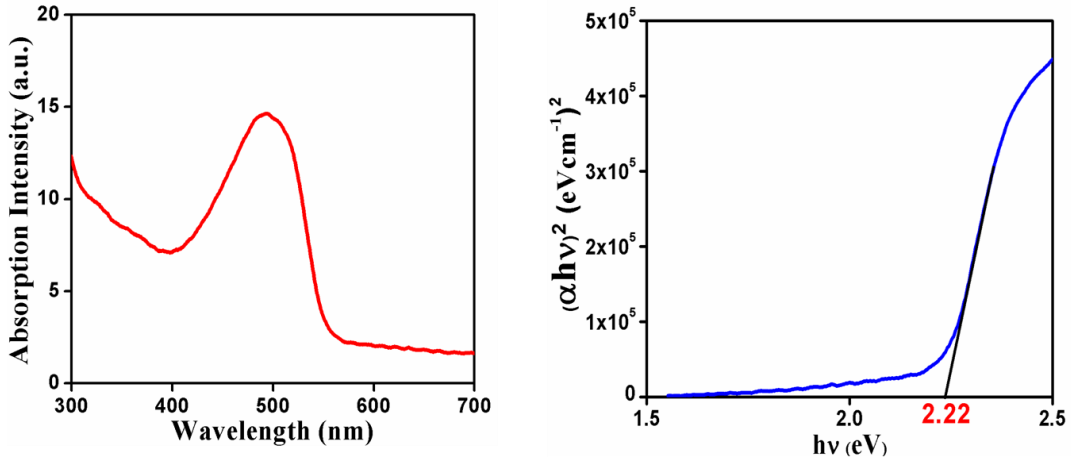

Figure 7: UV-vis absorption and Tauc's plot of MEH-PPV

V. FABRICATION OF DEVICE

5.1. Preparation of Active Composite (MEH-PPV/ZnO)

To explore the optical and electrical characteristics of the active material, solutions of MEH-PPV and ZnO nanoparticles with distinct morphologies labeled as (a), (b), and (c) were individually prepared in chloroform medium. The concentrations were set at 1.5 mg/mL for MEH-PPV and 0.3 mg/mL for each of the ZnO nanoparticle solutions. Each solution underwent sonication for 10 minutes at room temperature. Subsequently, MEH-PPV and ZnO nanoparticles were combined in an appropriate weight ratio of 2:0.1 to create the desired composite, and the mixture was sonicated for an additional 40 minutes. This process resulted in the preparation of three distinct active composites for the fabrication of thin active layers.

5.2. Photosensitivity of the composites

To evaluate this, the dark conductivity and photoconductivity of the MEH-PPV/ZnO composites were measured using a thin film technique, and the results are outlined in Table I. Thin films of each active composite were prepared on ITO-coated substrates through the spin-coating technique. The current density was recorded using a Keithley 2400 sourcemeter at various applied potentials, and photo illumination was provided by white light with an intensity of 80 mWcm-2. The incorporation of sphere-like ZnO nanoparticles with the polymer (MEH-PPV) resulted in a significant alteration of both the photosensitivity and the photoconducting properties of the blended composite.

ISSN (Print) : 2320 – 3765
ISSN (Online): 2278 – 8875

International Journal of Advanced Research in Electrical, Electronics and Instrumentation Engineering

(A High Impact Factor, Monthly, Peer Reviewed Journal, (An UGC Approved Journal))

Website: www.ijareeie.com

Vol. 6, Issue 9, September 2017

Table I: Conductivity and photosensitivity of the organic-inorganic composites

Sample	Dark Conductivity X 10^{-3} (Scm^{-1})	Photo Conductivity X 10^{-3} (Scm^{-1})	Photo Sensitivity
MEH-PPV	**7.38**	**12.08**	**1.64**
MEH-PPV/ZnO (Rod)	**12.28**	**151.78**	**12.36**
MEH-PPV/ZnO (Sphere)	**12.52**	**182.82**	**14.60**
MEH-PPV/ZnO (Flower)	**14.52**	**127.02**	**8.74**

In the case of a sphere-like structure, this area is maximized. The flower-like morphology, formed through the amalgamation of various ZnO particles, exhibits a larger apparent surface area compared to the sphere and rod-like morphologies. However, the effective junction area between the polymer and ZnO nanoparticles is significantly larger for the sphere-like morphology. Consequently, the composite material MEH-PPV:ZnO(NP) with a sphere-like morphology emerges as the most suitable candidate for the application in hybrid solar cells. This is attributed to the substantial improvement in the photo-induced current.

5.3. Fabrication Technique and Characterizations

To prepare the active layer, a thin, transparent buffer layer of PEDOT:PSS was spin-coated on the cleaned ITO-coated glass substrate, followed by drying at 70°C under a vacuum oven. Once the substrate was prepared, the pre-prepared solutions of the active composite MEHPPV:ZnO (nanoparticles of different morphology) were spin-coated onto the PEDOT:PSS film at a spinning rate of 1200 rpm for 2 minutes. The resulting film was obtained and dried in a vacuum desiccator at room temperature for 36 hours. For the top contact, an aluminum electrode was deposited through thermal evaporation using a shadow mask. With the completion of the devices, having the structure ITO/PEDOT:PSS/MEHPPV:ZnO/Al (schematic presentation provided below), further characterization was necessary.

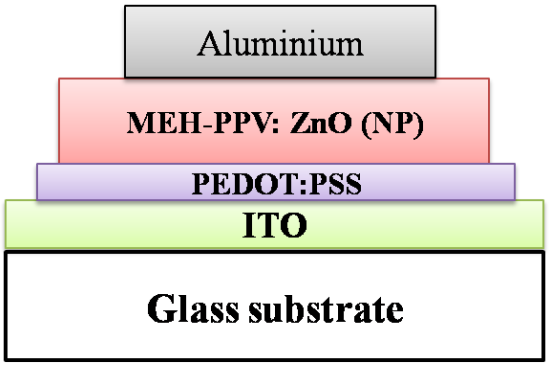

Scheme 1: Schematic presentation of MEH-PPV:ZnO based hybrid solar cell

VI. DEVICE CHARACTERIZATIONS

The current density-voltage (J-V) characteristics of the respective cells were measured using a Keithley 2400 source meter interfaced with a PC. The (J-V) characteristics of the devices, namely ITO/PEDOT:PSS/MEHPPV:ZnO flower-like NP/Al, ITO/PEDOT:PSS/MEHPPV:ZnO sphere-like NP/Al, and ITO/PEDOT:PSS/MEHPPV:ZnO rod-like NP/Al, were assessed under incident white light illumination with an intensity of 80 mWcm-2. Figure 8 illustrates the J-V characteristic curves of each device, and the effective surface area of the active device, fabricated through masking, is considered as 7.065 × 10-2 cm2.

ISSN (Print) : 2320 – 3765
ISSN (Online): 2278 – 8875

International Journal of Advanced Research in Electrical, Electronics and Instrumentation Engineering

(A High Impact Factor, Monthly, Peer Reviewed Journal, (An UGC Approved Journal))

Website: www.ijareeie.com

Vol. 6, Issue 9, September 2017

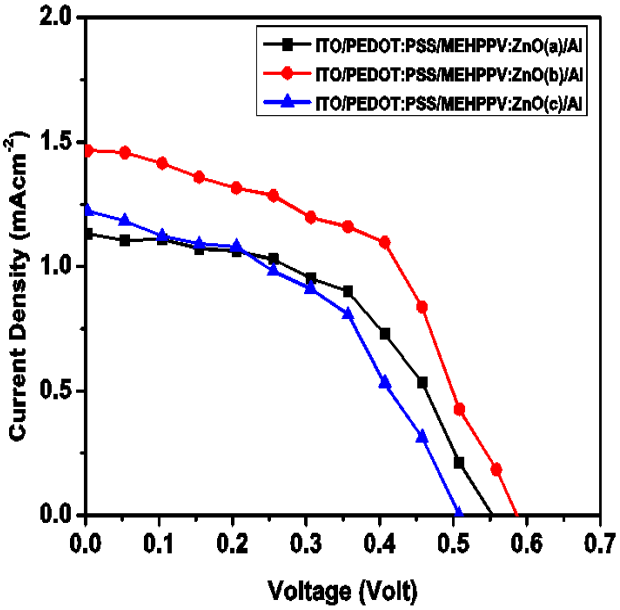

Figure 8: J-V characteristic of ITO/PEDOT:PSS/MEHPPV:ZnO(a) (rod-like) /Al, ITO/PEDOT:PSS/MEHPPV:ZnO(b) (sphere-like) /Al and ITO/PEDOT:PSS/MEHPPV:ZnO(c) (flower- like) /Al solar cells.

Table-I provides the measured values for open circuit voltage (VOC) and short circuit current density (JSC) obtained from the J-V characteristic curves. The corresponding efficiency (η) and fill factor (FF) for the devices were measured as 0.40%, 0.55%, 0.45% and 0.51, 0.51, 0.58, respectively. in this investigation, contribute to an improved absorption capacity of conjugated materials with MEH-PPV. This enhancement can potentially increase the generation rate of excitons.

Table II: Characteristic parameters of the active devices

Sample	V_{OC}	J_{SC}	V_{max}	J_{max}	FF	Efficiency
MEH-PPV/ZnO(Flower) based HSC	**0.555**	**1.131**	**0.357**	**0.899**	**0.51**	**0.051**
MEH-PPV/ZnO(Sphere) based HSC	**0.587**	**1.461**	**0.408**	**1.081**	**0.53**	**0.069**
MEH-PPV/ZnO(Rod) based HSC	**0.508**	**1.229**	**0.299**	**1.197**	**0.57**	**0.056**

The incorporation of sphere-like ZnO within MEH-PPV was expected to reduce bulk resistance, influenced by film thickness and controlled to some extent by morphology. Despite the initial anticipation that ZnO rod-like structures would enhance transport properties, the measured Jsc from the J-V characteristic demonstrated a contradiction, likely due to the random alignment of nanorods. The solar cell's performance relies significantly on the interface quality and energy quenching between donor and acceptor materials, associated with the band gap energy and absorption capabilities of nano-inorganic materials. Modifying the band gap of the inorganic acceptor material, particularly by altering the position of the LUMO energy level through controlled crystal growth during synthesis, is an avenue for improving VOC. According to Shockley and Queisser, VOC is directly linked to the energy difference between the

ISSN (Print) : 2320 – 3765
ISSN (Online): 2278 – 8875

International Journal of Advanced Research in Electrical, Electronics and Instrumentation Engineering

(A High Impact Factor, Monthly, Peer Reviewed Journal, (An UGC Approved Journal))

Website: www.ijareeie.com

Vol. 6, Issue 9, September 2017

LUMO of the acceptor and the HOMO of the donor material. The flower-like morphology exhibited a higher band gap energy than the rod-like structure, aligning with the Burstein–Moss theory. Depending on the morphological growth of semiconducting nanoparticles, the absorption edge shifts to higher energies, influencing the difference between the LUMO energy level of flower-like ZnO and the HOMO energy level of MEH-PPV, confirming the increase in VOC compared to devices with rod-like nanoparticles.

The formation of successive heterojunctions between organic donors and inorganic acceptors significantly affects current density, contingent on the homogeneity of composite materials. Homogeneity is influenced by the dispersity of inorganic nanoparticles with their morphological identity and functional groups. In this study, the sphere-like morphology exhibited high dispersion in chloroform without detectable agitation, confirmed by sharp FTIR spectra. Thus, it had the highest potential to form successive heterojunctions with the donor polymer in both solution and thin film, as observed in the performance. Photoluminescence spectra demonstrated successive static energy quenching, affirming enhanced charge transportation for the MEHPPV:ZnO sphere-like composite.
It is crucial to note that higher series resistance reduces the fill factor (FF). The improved fill factor for the device fabricated with rod-like ZnO nanoparticles indicated lower film resistance compared to the device with flower-like ZnO. In this experimental study, VOC and efficiency were enhanced for the device with sphere-like ZnO nano-semiconducting acceptors due to their lower bulk resistance influenced by morphology. Meanwhile, the VOC and efficiency of the device with flower-like ZnO improved compared to the device with rod-like ZnO nano-material, attributed to its higher absorption with a lower band gap.

Summary

Morphologies of ZnO nano-semiconducting materials (flower-like, sphere-like, and rod-like) were sequentially synthesized using the solvothermal technique with different capping reagents. Among these, the sphere-like morphology exhibits superior architecture with nano dimensions and enhanced light-absorbing properties. The optical, thermal stability, and photo-induced electrical properties of these synthesized materials were investigated when incorporated with the MEH-PPV donor polymer material. The photo-sensitivity of MEHPPV increased significantly due to the incorporation of sphere-like ZnO. The study concludes that the sphere-like structure of ZnO, owing to its high photo-sensing behavior, is more suitable for applications in MEH-PPV:ZnO-based organic-inorganic hybrid solar cells compared to rod and flower-like structures. The organic-inorganic hybrid solar cell configured with MEH-PPV:ZnO sphere-like morphology achieves the highest efficiency, along with improved Jsc and Voc. This is attributed to the formation of successive junctions between the organic donor and inorganic acceptor, facilitated by the structural symmetry and small particle size of sphere-like ZnO, coupled with its moderate absorption with band gap energy.

REFERENCES

[1] C. Kligshirn, *Phys. Status Solidi. B* 71 (1975) 547
[2] C. X. Ji, P.C. Searson, *J. Phys. Chem. B* 107 (2003) 4494.
[3] N. Saito, H. Haneda, T. Sekiguchi, N. Ohashi, I. Sakaguchi, and K. Koumoto, *Adv. Mater*. 14 (2002) 418.
[4] S. Liang, H. Sheng, Y. Liu, Z. Huo, Y. Lu, and H. Shen, *J. Cryst Growth* 225 (2001) 110.
[5] D.D. Lee, D.S. Lee, *IEEE Sensors J.* 1 (2001) 21
[6] J.X. Wang, X.W. Sun, A. Wei, Y. Lei, X.P. Cai, C.M. Li, and Z.L. Dong, *Appl. Phys. Lett.* 88 (2006) 233106.
[7] S.P. Singh, S.K. Arya, P. Pandey, B.D. Malhotra, S. Saha, K. Sreenivas, and V. Gupta, *Appl. Phys. Lett.* 91 (2007) 1
[8] J. Xu, Q. Pan, Y. Shun, *Sensors Actuator B* 66 (2000) 27.
[9] L. Fan, D. Yanhui, Y. Chen, L. Chen, J. Zhao, and P. Wang, *Solar Energy Materials & Solar Cells* 97 (2012) 64
[10] H.P. Fang, I.H. Chiang, C.W. Chu, C.C. h. Yang, and H.C. Lin, *Thin Solid Films*,519, Issue 15 (2011) 5212
[11] Jan Mescher*et al. Appl. Phys. Lett.* 101 (2012) 073301
[12] V.A.L. Roy, A.B. Djurisic,W.K. Chan, J. Cao, H.F. Lui, and C. Surya, *Appl. Phys. Lett.* 83 (2003) 14
[13] Q.H. Chen, W.G. Zhang, *J. Non-cryst. Solids* 353 (2007) 374
[14] W.J.E.Beek, M. M.Wienk, A. Rene.and J.Janssen, *Adv.Mater.* 2004,6,No. 12,June 17.
[15] S. VenkataprasadBhat, A. Govindaraj, and C.N.R. Rao, *Solar Energy Materials and Solar Cell*, 95 (2011) 2318
[16] Y. Chen, D.M. Bagnall, H. Koh, K. Park, K. Hiraga, Z. Zhu, and T. Yao, *J. Appl. Phys.* 84 (1998) 3912

ISSN (Print) : 2320 – 3765
ISSN (Online): 2278 – 8875

International Journal of Advanced Research in Electrical, Electronics and Instrumentation Engineering

(A High Impact Factor, Monthly, Peer Reviewed Journal, (An UGC Approved Journal))

Website: www.ijareeie.com

Vol. 6, Issue 9, September 2017

[17] C.T. That, R. Matthew. T Philips, and P. Nguyen, *Journal of Luminescence*, 128 (2008) 2031
[18] Y. Abdollahi, A. H. Abdullah1, Z. Zainal1, and N. A. Yusof, *International Journal of Basic & Applied Sciences*, 11 (2011)118104.
[19] P.Chakraborty, G.Datta and K.Ghatak , *Physica Scripta***,** 68 (2003) 368.
[20] J. Zhang, *Chem. Mater*. 14 (2002) 4172
[21] X. Gao, X. Li, andW. Yu, *J. Solid State Chem.* 178 (2005) 1139
[22] H. Zhang, D. Yang, D. Li, X. Ma, S. Li, and D. Que, *Cryst. Growth Designe* 5 (2005) 547
[23] G. Yuan, Z. Ye, L. Zhu, J. Huang, Q. Qian and B. Zhao, *J. Cryst. Growth* 268 (2004) 169
[24] K. Ip, Y. W. Heo, K. H. Baik, D. P. Norton, S. J. Pearton, S. Kim, J. R. LaRoche and F. Ren, *Appl. Phys. Lett.* 84 (2004) 2835
[25] J. Zhang, et al. *Chem. Mater*. 14 (2002) 4172
[26] X. Gao, X. Li and W. Yu, *J. Solid State Chem.* 178 (2005) 1139
[27] H. Zhang, D. Yang, D. Li, X. Ma, S. Li and D. Que, *Cryst. Growth Des.* 5 (2005) 547
[28] G. V. Seguel, B. L. Rivas, C. Novas, and J. Chil. *Chem. Soc.* 50 (2005) 401
[29] K.Morishige, S.Kittaka, and T.Moriyasu, *J.C.S.Faraday* 176 (1980) 728
[30] N. Z. Yahya and M. Rusop, *Journal of Nanomaterials Article ID 793679*, 4 (2012) doi:10.1155/2012/793679
[31] Y.Z.Lee, X.Chen, S.A.Chen, P. K.Wei and W. S. Fann, *J. Am. Chem. Soc.* 123 (2001) 2296
[32] W.Shockley and H. Queisser, *J. Appl. Phys.* 32 (1961) 510
[33] Y. Abdollahi, A. H. Abdullah, Z. Zainal, and N. A. Yusof, *International Journal of Basic & Applied Sciences*, 11 (2011) 62
[34] P. Chakraborty, G. Datta, and K. Ghatak, *Physica Scripta* 68 (2003) 368
[35] G.Yu and A.J.Heeger, *J.Appl.Phys.* 78 (1995) 4510
[36] J.Yu, D.Hu, and P.F.Barbara, *Science* 289 (2000) 1327
[37] Y.Kang and D.Kim, *Scl. Energy Mater. Sol. Cells* 90 (2006)166